

## PRECISE COMPUTER MODELS OF THE INDUCTION MACHINE IN THE MATLAB/SIMULINK

**Introduction.** Thanks to their reliable design, low cost and the ease in starting and reversal, induction motors (IM) have wide application in the unregulated electric drives (ED) of common industrial mechanisms. Recently, as a result of swift development in rapid power semiconductor and microelectronic technology, IM also gain the areas of precision and dynamic adjustable ED where previously only DC ED were used. To develop effective systems for vector control of induction ED we must have an adequate enough mathematical model of the IM, the development of which has been the goal of many studies for almost a century.

**The problem under investigation.** The computer software MatLab/Simulink is a powerful modern resource for research on the development of electronic control systems for ED. The virtual computer models of electrical machines are presented in one of the libraries SimPowerSystem. The available models of IM with squirrel-cage as well as with a wound rotor can be represented in different coordinate systems, but only as an idealized machine, for which one adopts a significant number of known assumptions [1]. For many modes of IM, some of these assumptions may be far from reality, which will bring in significant errors in the operation of the control systems or will disable them completely. Thus, one is faced with the problem of developing different variants of more precise computer models of IM. These models should take into account the major deviations from the ideal: losses in steel, magnetic saturation in the circle of main magnetic flux as well as of leakage flux in the circles of the stator and rotor, displacement of the current in the rotor circle, etc.

**The basic computer model of the idealized IM.** To develop a precise computer model, we must use such a mathematical description of the IM dynamics which will allow us the simplest way to take into account the different types of deviations from the idealized IM. They may be quite approximate in character; the main thing is to be able to account for these deviations, so that later we may use such models to develop and explore the robustness of control systems. The analysis of the known descriptions of IM permitted us to adopt for our basis the mathematical model of idealized IM in orthogonal  $d$ - $q$  coordinates which rotates with the arbitrary angular speed  $\omega$  [2]. Then, in the case of symmetric feeding power, electromagnetic processes in the IM are described by the following system of equations:

- electric balance equations

$$\begin{aligned} u_{ds} &= R_s i_{ds} + p\psi_{ds} - \omega\psi_{qs}; & u_{qs} &= R_s i_{qs} + p\psi_{qs} + \omega\psi_{ds}; \\ u'_{dr} &= R'_r i'_{dr} + p\psi'_{dr} - (\omega - \omega_r)\psi'_{qr}; & u'_{qr} &= R'_r i'_{qr} + p\psi'_{qr} + (\omega - \omega_r)\psi'_{dr}; \end{aligned} \quad (1)$$

- equations of fluxes

$$\begin{aligned} \psi_{ds} &= L_{\sigma s} i_{ds} + L_M (i_{ds} + i'_{dr}); & \psi_{qs} &= L_{\sigma s} i_{qs} + L_M (i_{qs} + i'_{qr}); \\ \psi'_{dr} &= L'_{\sigma r} i'_{dr} + L_M (i_{ds} + i'_{dr}); & \psi'_{qr} &= L'_{\sigma r} i'_{qr} + L_M (i_{qs} + i'_{qr}), \end{aligned} \quad (2)$$

where indices  $s$  and  $r$  reflect their belonging to the stator and rotor respectively; a bar shows the alignment of the rotor windings to the stator windings;  $p$  is the differentiation operator;  $u$ ,  $i$ ,  $\psi$  are the voltage, current, and flux respectively;  $R$  is the resistance;  $L_{\sigma}$ ,  $L_M$  are the leakage and magnetizing inductance respectively;  $\omega_r$  is the angular speed of rotor

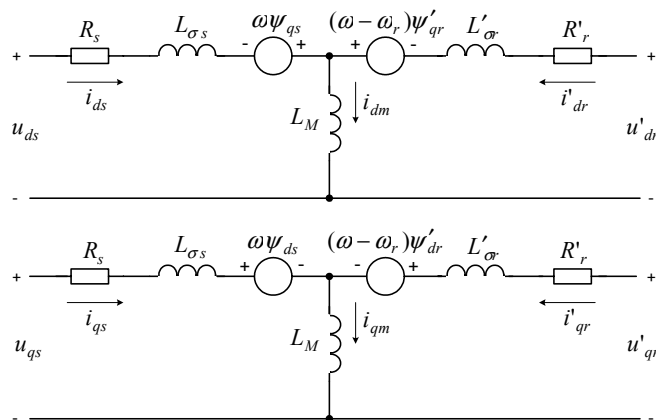


Fig. 1. The equivalent electric circuit that reflects the electromagnetic processes in the idealized IM

in the rad. el./sec.

Voltage (1) and flux (2) equations correspond to the equivalent electrical circuit (Fig. 1), which reflects the voltage balance in static and dynamic modes of idealized IM [2]. For squirrel-cage IM  $u'_{qr} = u'_{dr} = 0$ .

The electromagnetic torque can be expressed by the vector product of various combinations of fluxes or currents; for example, by one of the following equations:

$$\begin{aligned} T &= 1,5P(\psi_{ds}i_{qs} - \psi_{qs}i_{ds}); \\ T &= 1,5P(\psi'_{qr}i'_{dr} - \psi'_{dr}i'_{qr}); \\ T &= 1,5Pk_L(\psi'_{dr}i_{qs} - \psi'_{qr}i_{ds}), \end{aligned} \quad (3)$$

where  $P$  is the number of pairs of the IM poles, and  $k_L = L_M / (L'_{\sigma r} + L_M)$ .

For a general mathematical model of IM, one needs to add to equations (1)-(3) the equation of the mechani-

cal part, such as the one for the simplest case of the single mass kinematical system:

$$p\omega_{rm} = \frac{1}{J}(T - b\omega_{rm} - T_l), \quad (4)$$

where  $\omega_{rm} = \omega_r/P$  is the angular speed of IM,  $J$  is the total moment of inertia of ED, brought to the IM shaft,  $b$  is the ratio of total internal and external viscous friction, and  $T_l$  is the static load moment on the shaft of IM.

We can build the computer model of the idealized IM directly on the obtained complete nonlinear system of differential equations (1)-(4). The calculation algorithm may be as follows: in the electromagnetic part, by integrating we obtained the projections of fluxes from the equations (1); we then used these projections in the equations (2) for determining the current projections, which, in turn, are featured in equations (1). Due to the interrelationships between currents and fluxes in stator, rotor and between them, as well as to the cross-links between the equations of coordinate projections, the constructed system will adequately reflect the electromagnetic processes taking place in IM both in steady-state and in transient conditions. The electromagnetic torque is determined from one of the equations (3) using obtained values of fluxes and currents. Further, it takes part in the formation of the angular speed according to equations (4). The value of angular speed passes on to the electromagnetic part of the IM, where according to equations (1) it determines the values of emfs.

The computer model of the IM built in this way is shown in Fig. 2. To check it, we will conduct a simulation of the direct connection of IM to the industrial grid. To do this, we will use the coordinate system rotating with the angular speed of the magnetic field of the machine:  $\omega = 2\pi f_n = 314.16$  rad/s. In this case, the projections of supply voltage  $U_{ds}$  and  $U_{qs}$  will have permanent values, and it is not important what their specific values are, as long as the following condition is fulfilled:  $U_{ds}^2 + U_{qs}^2 = U_m^2 = 2U_{ns}^2 = 2 \cdot 220^2$  V<sup>2</sup>; let's assume, for example, that:  $U_{ds} = 0$ ,  $U_{qs} = 311$  V.

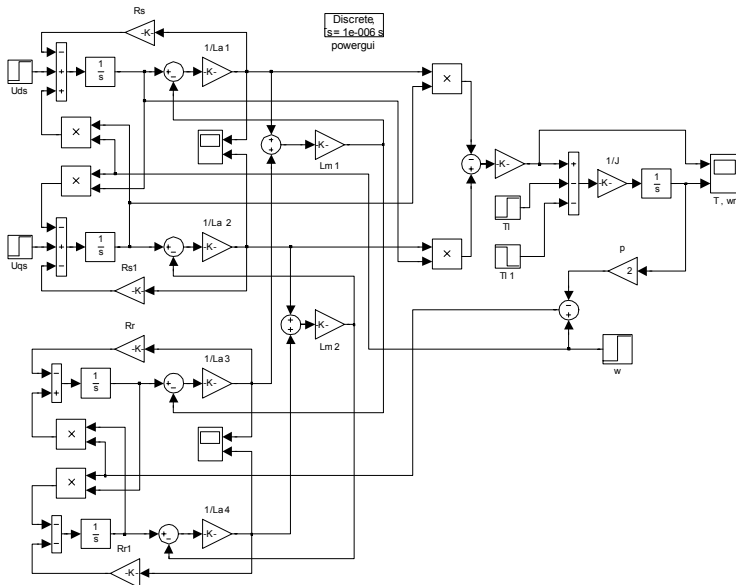


Fig. 2. The computer model of the stator voltage-controlled idealized IM

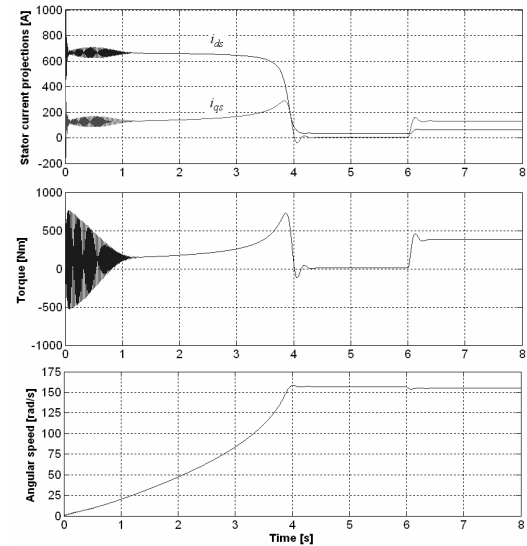


Fig. 3. The simulation waveforms of the stator current projections, electromagnetic torque and angular speed at the starting up of the idealized IM and the apposition of the rated load

For our research purposes, let's use the IM 4A225M2U3 with such nominal parameters [3]:  $R_n = 55$  kW,  $U_n = 380/220$  V,  $n_n = 1420$  rpm,  $I_n = 108$  A,  $J = 5.5$  kg·m<sup>2</sup>. The absolute values of winding parameters calculated on the basis of the relative values taken from the IM passport are:  $R_s = 0.055$  Ohm,  $R'_r = 0.0306$  Ohm,  $L_{\sigma s} = 0.5577$  mH,  $L'_{\sigma r} = 0.9078$  mH,  $L_M = 0.02723$  H. Fig. 3 shows the simulation waveforms of the main variables at the direct starting up of the IM (with no-load torque 10 N·m) and the subsequent apposition of rated load torque  $T_l = 360$  Nm at the moment 6 s.

**The computer model of the voltage-controlled IM that takes into account the iron losses.** For a simple and quite adequate mathematical modeling of iron losses in the steady-state mode of the IM, the equivalent resistance can be connected up in parallel to the magnetizing branch in the equivalent electric circuit. The value of this resistance can be determined experimentally in no-load machine condition. For instance, in [4] is used such an expression for the value of resistance in relative units which models the total iron losses:

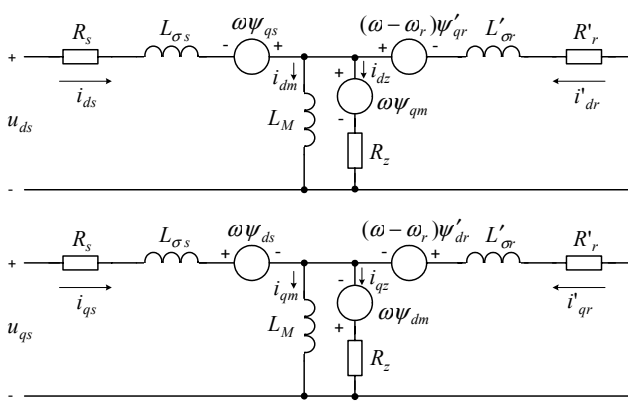


Fig. 4. The equivalent circuit that reflects the electromagnetic processes in the IM taking into account iron losses

In addition to the voltage balance equations (1), we should add to the model the equations for the two obtained circuits:

$$R_z i_{dz} = p \psi_{dm} - \omega \psi_{qm} ;$$

$$R_z i_{qz} = p \psi_{qm} + \omega \psi_{dm} ,$$

where  $\psi_{dm} = L_M i_{dm}$ ,  $\psi_{qm} = L_M i_{qm}$  are the  $d$ - $q$  axis projections of flux of the magnetizing branch of IM.

Also, we should consider the changes in the balances of currents in nodes:

$$i_{ds} + i'_{dr} = i_{dm} + i_{dz} ;$$

$$i_{qs} + i'_{qr} = i_{qm} + i_{qz} .$$

Out of the electromagnetic torque expressions (3) only the second one will obtain when we take into account the iron losses. It is based on rotor flux and current, that is, on the variables of the output part of the scheme.

Given the additional equations (6) and (7), the computer model of the idealized IM shown in Fig. 2 should be expanded by introducing yet another automatic control system with cross-connections, which reflects these additional equations (Fig. 5). Value of resistance  $R_z$  is calculated, for example, by expression (5) (if the relevant factors are known) in the subsystems  $R_z$ , the inputs of which receive the running values of  $f$  and  $s$ . In a simpler case, one may take the constant value of resistance  $R_z$ .

#### The computer model of the voltage-controlled IM that takes magnetic

**saturation into account.** There are many works devoted to the study and mathematical modeling of saturation in the IM, which use different approaches to the incorporation of the saturation of magnetic paths: for the main magnetic flux, for the leakage fluxes, only in the stator or rotor, or in both parts of the machine, cog saturation, etc. The main way of its modeling is based on the circuit patterns of IM with varying complexity [6,7]. However, there are other, more accurate methods, which have been compared in [8].

Given the advantages of mathematical modeling of the IM in rotating  $d$ - $q$  coordinates, we will use the basic electrical circuit to simulate saturation in the IM (Fig. 1). We satisfy saturation by nonlinear dependences of leakage inductances of stator and rotor, as well as the inductance of the magnetizing branch from currents. For this aim, we will use the methodology developed by Lipo [9]. According to it, stator and rotor leakage inductances have to be separated into

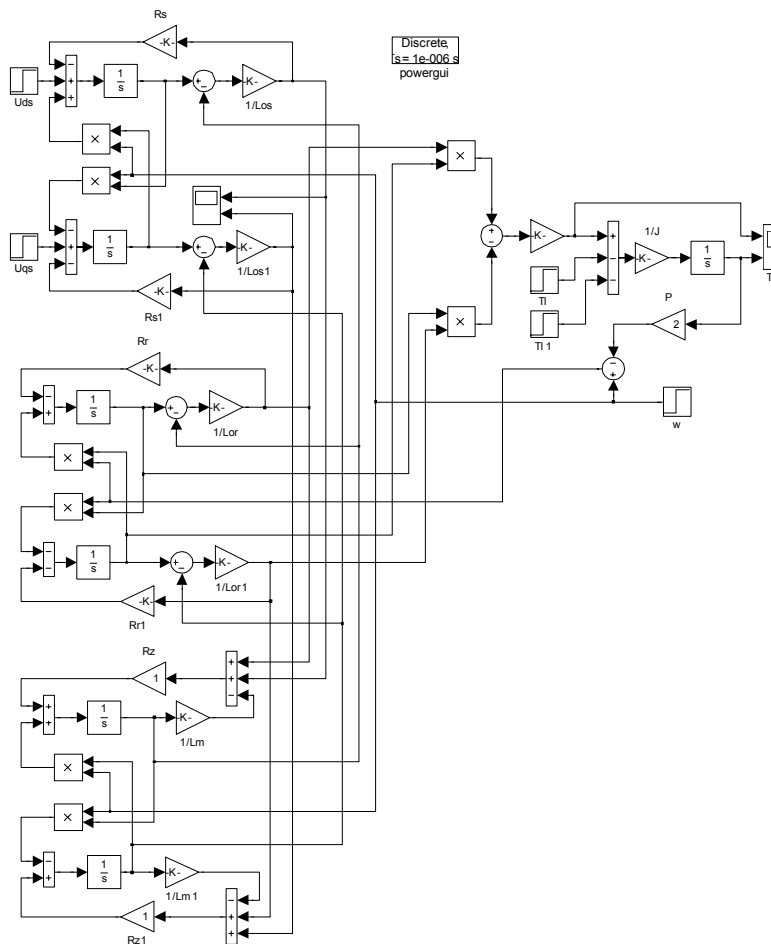


Fig. 5. The computer model of the stator voltage-controlled IM that takes into account the iron losses

two components – air-dependent  $L_{\sigma a}$  and iron-dependent  $L_{\sigma i}$ . The former reflect leakage fluxes in end-winding parts of the machine and are constant, and the latter reflect the sum of iron-dependent leakage fluxes in slots, belts and skew leakage for stator and rotor. Saturation is also considered when determining the magnetizing inductance  $L_M$ . The values of iron-dependent inductance are expressed through their excitation currents.

Based on the proposed conception, instead of (2) the fluxes in the IM will be expressed as follows:

$$\begin{aligned}\psi_{ds} &= (L_{\sigma as} + L_{\sigma is})i_{ds} + L_M(i_{ds} + i'_{dr}); & \psi_{qs} &= (L_{\sigma as} + L_{\sigma is})i_{qs} + L_M(i_{qs} + i'_{qr}); \\ \psi'_{dr} &= (L'_{\sigma ar} + L'_{\sigma ir})i'_{dr} + L_M(i_{ds} + i'_{dr}); & \psi'_{qr} &= (L'_{\sigma ar} + L'_{\sigma ir})i'_{qr} + L_M(i_{qs} + i'_{qr}).\end{aligned}\quad (8)$$

Each of the projections of fluxes (8) consists of a part that is linearly dependent on the current and of one that is nonlinearly dependent because of saturation. We will denote the latter as " $*$ ". For example, for the first equation (8)

$$\psi_{ds} = L_{\sigma as}i_{ds} + L_{\sigma is}i_{ds} + L_M(i_{ds} + i'_{dr}) = \psi_{ads} + \psi_{ids}^* + \psi_{dm}^*. \quad (9)$$

Thus, for computer modeling of saturation, the idealized model of the IM should be complemented with functional blocks, which simulate the magnetizing curves of main magnetic flux and leakage fluxes. To accomplish this, by means of integrating the basic equations (1), we determine the full fluxes  $\psi_{ds}$ ,  $\psi_{qs}$ ,  $\psi'_{dr}$ ,  $\psi'_{qr}$ . The projections of the stator and rotor currents are calculated by the expressions of balance of fluxes (8) taking into account their nonlinear type (9):

$$\begin{aligned}i_{ds} &= \frac{1}{L_{\sigma as}}(\psi_{ds} - \psi_{ids}^* - \psi_{dm}^*); & i_{qs} &= \frac{1}{L_{\sigma as}}(\psi_{qs} - \psi_{iqs}^* - \psi_{qm}^*); \\ i'_{dr} &= \frac{1}{L'_{\sigma ar}}(\psi'_{dr} - \psi'_{idr}^* - \psi_{dm}^*); & i'_{qr} &= \frac{1}{L'_{\sigma ar}}(\psi'_{qr} - \psi'_{iqr}^* - \psi_{qm}^*).\end{aligned}$$

To obtain the mathematical description of saturation with high precision, we model the magnetizing curve using the arctangent function [6]:

$$\psi = a_1 \arctan(a_2 i) + a_3 i, \quad (10)$$

where  $a_1, a_2, a_3$  are the coefficients that are obtained from the experimentally determined magnetizing curve.

Thus, having obtained the dependence  $U_s(I_s)$  in locked-rotor and no-load tests respectively on the main frequency ( $\omega_b = 314$  rad/s), we determine the nonlinear fluxes in accordance with the following expressions, assuming that stator flux and rotor flux converted to the stator are equal [6]:

$$\begin{aligned}\psi_{\sigma is}^* &= \psi_{\sigma ir}^* = \frac{1}{\sqrt{6}} \frac{U_s}{\omega_b}; \\ \psi_m^* &= \sqrt{\frac{2}{3}} \frac{U_s}{\omega_b}.\end{aligned}\quad (11)$$

From these dependences  $\psi(I)$ , coefficients  $a_1, a_2, a_3$  can be obtained by using the method of the smallest squares.

In the model of the investigated IM, we assume the following roughly estimated

values of parameters:  $L_{\sigma as} = 0.11$  mH,  $L'_{\sigma ar} = 0.18$  mH. To determine the fluxes that are nonlinearly dependent on the relevant currents, we use expressions like (10) with the same coefficients for projections  $d$  and  $q$ :

$$\psi_{is}^* = 0,254 \arctan(1,77 \cdot 10^{-3} i_s); \quad \psi_{ir}^* = 0,412 \arctan(1,77 \cdot 10^{-3} i_r); \quad \psi_m^* = \arctan(0,03 i_m). \quad (12)$$

This computer model is shown in Fig. 6, where nonlinear fluxes (12) depending on the relevant currents are calculated in the subsystems Li1-Li6.

The electromagnetic torque that takes saturation into account can be defined similarly to expressions (3), but using only nonlinear fluxes like (12), for example:  $M = 1,5P(\psi_{qs}^* i_{ds} - \psi_{ds}^* i_{qs})$ .

**The computer model of the voltage-controlled IM that takes into account the current displacement in rotor.** Displacement of current in the rotor windings, placed in deep slots to increase the starting torque, can be easily taken

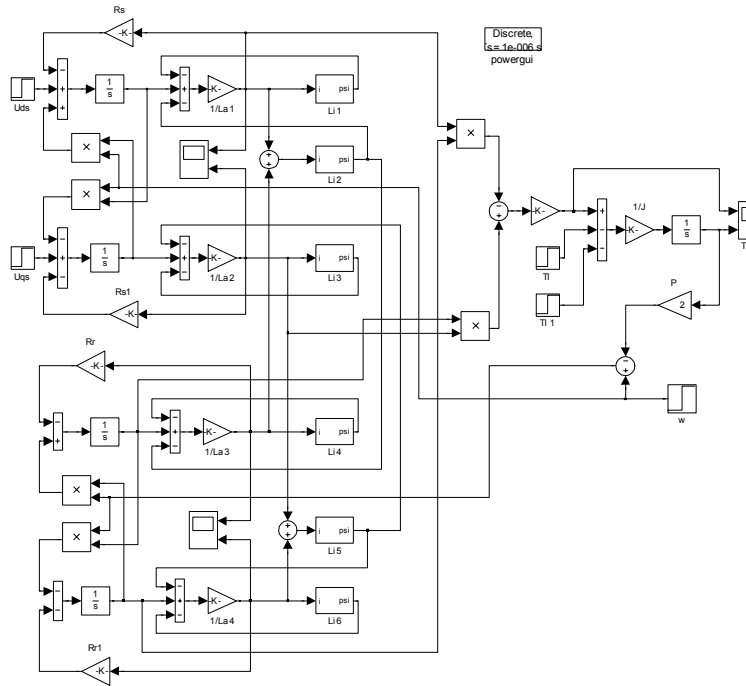


Fig. 6. The computer model of stator voltage-controlled IM that takes saturation into account

into account in the basic computer model of the idealized IM (Fig. 2), entering the dependences of rotor resistance and leakage inductance converted to stator on the displacement of current:

$$R'_r = k_r R'_{r.sl} + R'_{r.br} ; \quad L'_\sigma r = k_l L'_{\sigma r.sl} + L'_{\sigma r.br} , \quad (13)$$

where the indices *sl* and *br* mark the converted to stator resistance and leakage inductance of slot and end-winding parts of the rotor winding respectively,  $k_r$  and  $k_l$  are the factors that account for the change in the slot parts of active resistance and leakage inductance in the rotor winding during the displacement of current respectively.

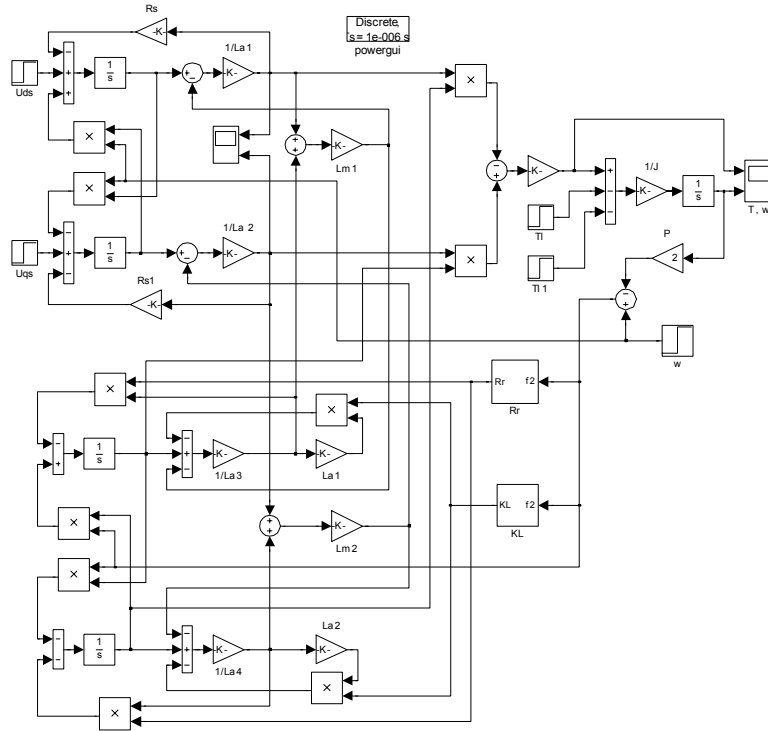


Fig. 7. The computer model of the stator voltage-controlled IM that takes into account current displacement in rotor

The factors  $k_r$  and  $k_l$  can be obtained with sufficient precision using the known expressions [10]:

$$k_r = \xi \frac{\text{sh } 2\xi + \sin 2\xi}{\text{ch } 2\xi - \cos 2\xi} ;$$

$$k_l = \frac{3}{2\xi} \frac{\text{sh } 2\xi + \sin 2\xi}{\text{ch } 2\xi - \cos 2\xi} , \quad (14)$$

where  $\xi = 2\pi h_r \sqrt{\frac{b_r f_2}{b_s \rho_r}} \cdot 10^{-7}$  ;  $h_r$  is

the height of conductive rod in a slot,  $b_r$  and  $b_s$  are the rod width and slot width respectively,  $f_2$  is the current frequency in the rotor, and  $\rho_r$  is the resistivity of rod material.

In the computer model of the IM that takes into account current displacement (Fig. 7), unlike in the basic computer model, in subsystem *Rr* and *Lr* we calculate  $R'_r$  and  $k_l$  using expressions (13) and (14) depending on  $f_2 = (\omega - \omega_r)/(2\pi)$ . For the investigated IM with aluminum rods of the rotor cage, the following parameters are accepted:  $R'_{r.sl} = 0.0206$  Ohm,

$$R'_{r.br} = 0.01 \text{ Ohm}, \quad L'_{\sigma r.sl} = 0.8078 \text{ mH}, \quad L'_{\sigma r.br} = 0.1 \text{ mH}, \quad h_r = 0.032 \text{ m}, \quad b_r/b_s = 1.$$

**The results of computer simulation.** Fig. 8, a, b, c gives the simulated waveforms at startup and subsequent apposition of the rated torque for the investigated IM, similar to those shown in Fig. 3 for the idealized IM, but taking into account iron losses, saturation and current displacement in rotor performed on computer models, shown respectively in Fig. 5, 6, and 7. The resistance value that models iron losses is taken as the constant  $R_z = 1.0$  Ohm. Compared to the idealized IM, taking iron losses into account leads to changes of the stator current projection  $i_{qs}$ , which increased from 150 up to 250 A, while the projection  $i_{ds}$  remains unchanged and equal to 660 A. This is because the direction of stator voltage vector in rotating coordinates was chosen along the axis  $q$  ( $U_{ds} = 0$ ). The values of the electromagnetic torque decreased significantly (the range of fluctuations at the beginning of startup, instantaneous values after oscillations and the maximum), resulting in the startup time increase from 4.0 s to 4.32 s. Compared to the idealized IM, taking saturation into account leads to a substantial increase of current projections of the stator, the range of fluctuation, and instantaneous values of the electromagnetic torque, and hence to almost as twice fast startup of the IM. Displacement of current in the rotor causes any stator current reduction compare with the saturation case, while the starting torque significantly increases resulting in the startup time reduces to 2 s. Fig. 8, d gives the simulated waveforms, when in model we take into account both a saturation and current displacement in rotor. In this case stator current and torque increase significantly and startup time still reduces to almost 1 s.

**Conclusions.** Using the mathematical model of the idealized IM in orthogonal coordinate system that rotates with arbitrary angular speed as a basis for computer simulation makes it relatively easy to refine it, taking into account iron losses, saturation of the main magnetic path and paths of leakage of the magnetic flux in stator and current displacement in the rotor. It also makes it possible to account for different combinations of these three factors in a single computer model.

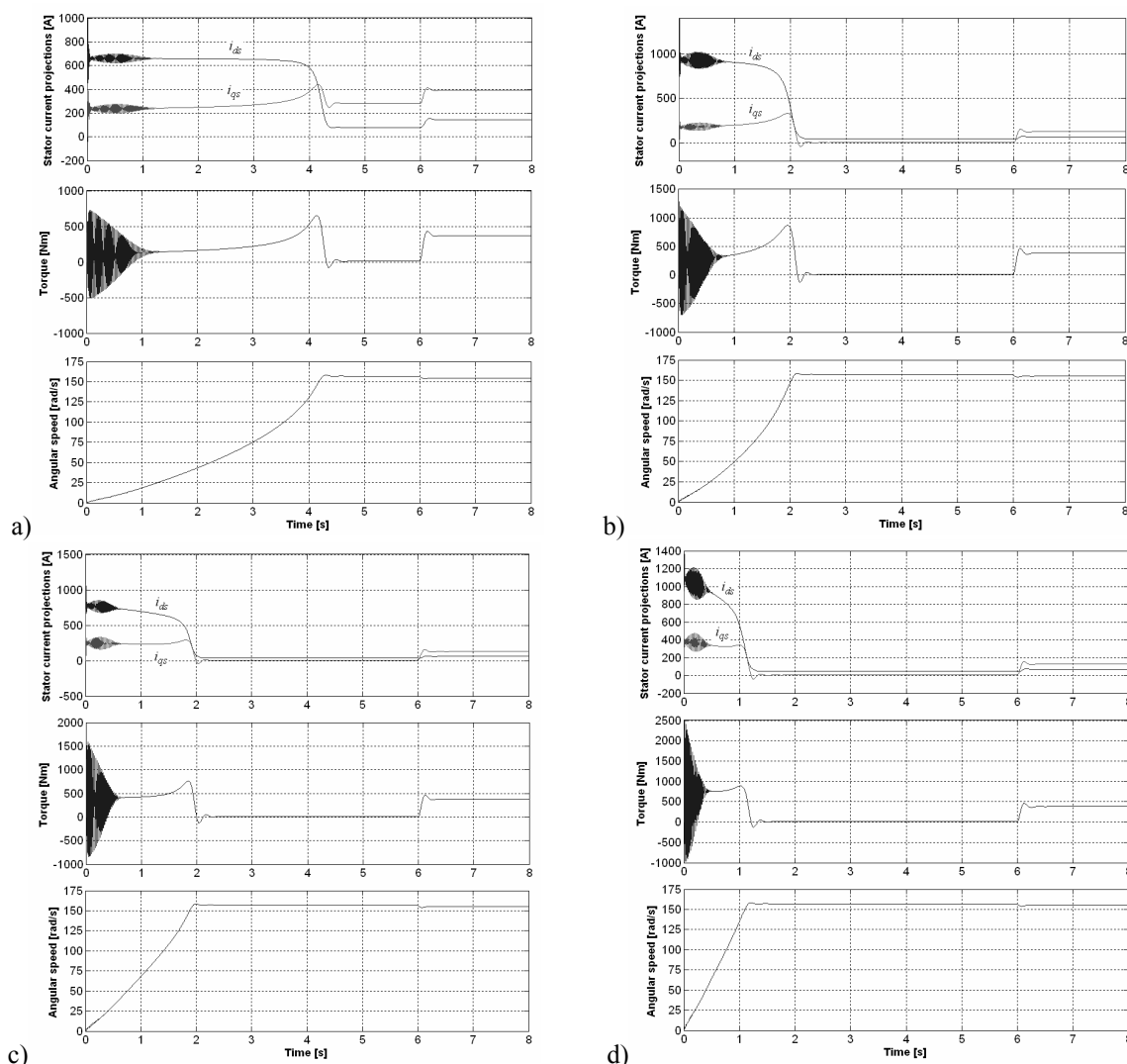


Fig. 8. Simulated waveforms of the stator currents, torque and angular speed at startup, and apposition of the rated load for the IM taking into account: a) iron losses, b) saturation, c) current displacement in the rotor, d) both saturation and current displacement in the rotor

## References

1. Пивняк Г.Г., Волков А.В. Современные частотно-регулируемые асинхронные электроприводы с широтно-импульсной модуляцией. – Днепропетровск: НГУ, 2006. – 470 с.
2. Krause P.C., Wasynczuk O., Sudhoff S.D. Analysis of Electric Machinery and Drive Systems. – Wiley-Interscience, 2002. – 606 p.
3. Асинхронные двигатели серии 4А: Справочник .. А.Э.Кравчик, М.М.Шлаф, В.И.Афонин, Е.А.Соболевская. – М.: Энергоатомиздат, 1982. – 504 с.
4. Kirschen D.S., Novotny D.W., Suwanwisot W. Minimizing induction motor losses by excitation control in variable frequency drives // IEEE Trans. on Industr. Appl., 1984, Vol. IA-20, No. 5, pp. 1244–1250.
5. Wee S.-D., Shin M.-Ho., Hyun D.-S. Stator-flux-oriented control of induction motor considering iron loss // IEEE Trans on Industr. Electron., 2001, Vol. 48, No. 3, pp. 602–608.
6. Keyhani A., Tsai H. Ispice simulation of induction machines with saturable inductances // IEEE Trans. on Energy Convers., 1989, Vol. 4, No. 1, pp. 118–125.
7. Ojo J.O., Consoli A., Lipo T.A. An improved model of saturated induction machines // IEEE Trans. on Industr. Appl., 1990, Vol. 26, No. 2, pp. 212–221.
8. Sudhoff S.D., Aliprantis D.C., Kuhn B.T., Chapman P.L. An induction machine model for predicting inverter-machine interaction // IEEE Trans. on Energy Convers., 2002, Vol. 17, No. 2, pp. 203–210.
9. He Yi-K., Lipo T.A. Computer simulation of an induction machine with spatially dependent saturation // IEEE Trans. on Power Appar. and Syst., 1984, Vol. PAS-103, No. 4, pp. 707–714.
10. Проектирование электрических машин / И.П.Копылов, Ф.А.Горяинов, Б.К.Клоков и др. – М.: Энергия, 1980. – 496 с.